TU Clausthal

Clausthal University of Technology

Classical Beam Theory with Arbitrary Number of Layers

Stefan Hartmann, Pranav Kumar Dileep

Technical Report Series

Fac3-19-02

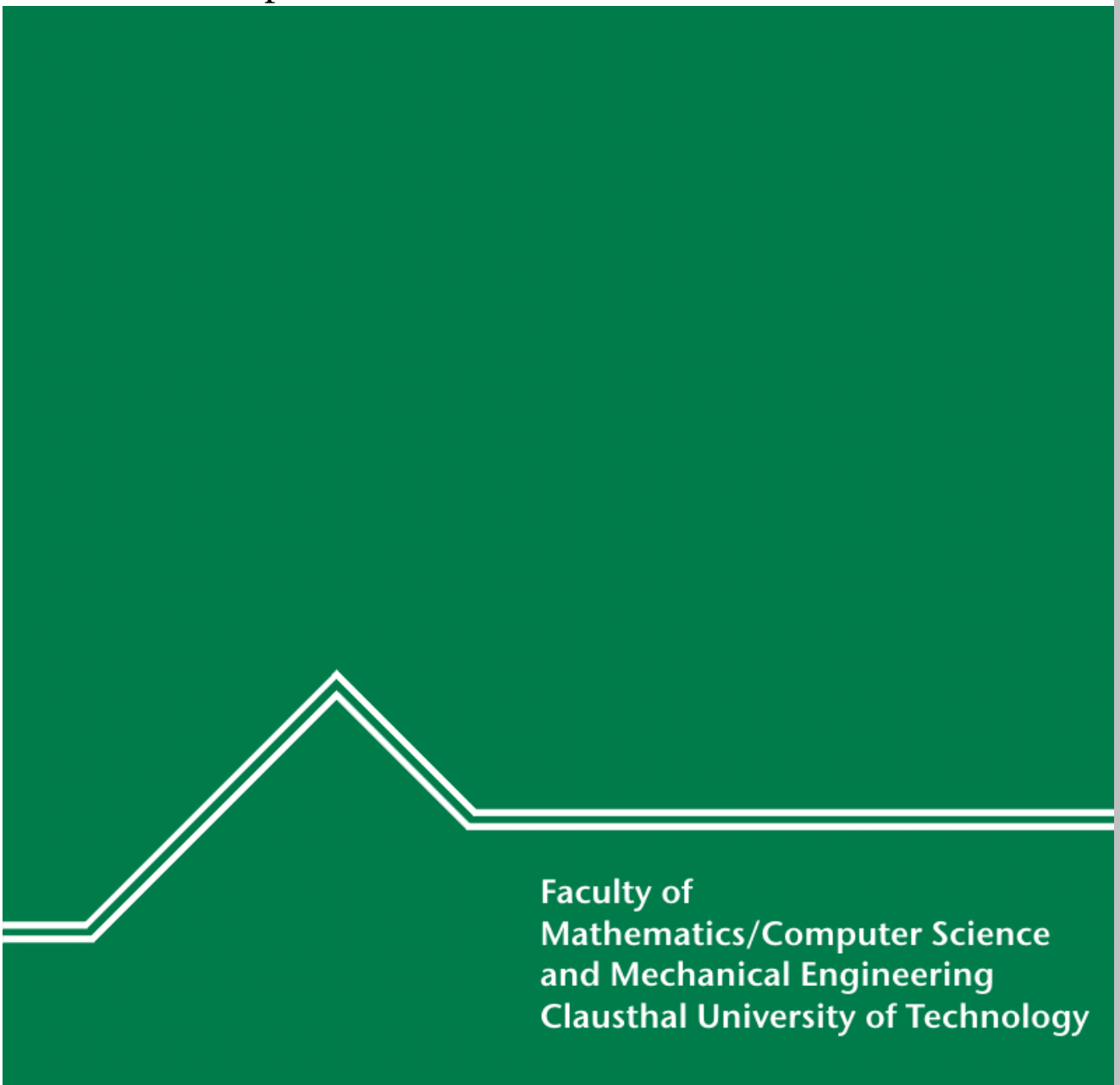

Impressum

Publisher: Fakultät für Mathematik/Informatik und Maschinenbau,
Technische Universität Clausthal
Agricolstr. 2, 38678 Clausthal-Zellerfeld, Germany
Editor-in-chief: Volker Wesling
Technical editor: Martina Wächter
Contact: martina.waechter@tu-clausthal.de
URL: http://www.fakultaet3.tu-clausthal.de/forschung/technical-reports/
ISSN: 1869-8018

The Faculty of Mathematics/Computer Science and Mechanical Engineering Review Board

Classical Beam Theory with Arbitrary Number of Layers

Stefan Hartmann and Pranav Kumar Dileep

Institute of Applied Mechanics, Clausthal University of Technology, Clausthal-Zellerfeld, Germany

Classical Beam Theory with Arbitrary Number of Layers

Abstract

This short essay treats a bending theory for long beams made from laminates, i.e. a beam theory is derived for linear, elastic, isotropic material at small strains. It is a generalization to an arbitrary number of layers. As an example layered steel-polymer-steel (SPS) laminates are looked at, which are treated in metal-polymer-metal (MPM) bending forming processes, where the stress state influences the failure behavior.

1 Introduction

A beam is a common structural member which resists the influence of applied lateral load by bending. Generally, the cross-sectional dimensions of the beam are small when compared to its length. Beams are made-up of several materials and commonly used among them are metals, alloys, wood, concrete etc. This might be for example in timber industry, where various kinds of wood are glued together, see (Leichti et al., 1990), or applications with bimetallic strips, see (De Vries and Lauderbaugh, 1984). Fiber reinforced composite plies are arranged as layered fabrics which form a laminate. Commonly, the width of the laminates is large in comparison to its height so that plate theory is of more of interest in these cases. Additional applications are in metal forming industry, where thin metal sheets are combined with a polymer core, (Burchitz et al., 2005; Hufenbach et al., 2008; Harhash et al., 2018). Multi-layered beams are also known as sandwich beams, which frequently are used in aircraft and construction industries due to its high stiffness-strength ratio. Thus, a beam theory gives a first insight into the basic stress state.

The mechanics of simple beams are explained using classical beam theories, namely, Timoshenko beam theory (Timoshenko, 1921, 1922) and Euler-Bernoulli beam theory (Euler, 1744), for more information on classical and advanced theories of beams, refer (Carrera et al., 2011). Comparison of various linear beam theories can also be found in (Labuschagne et al., 2009). Apart from the estimation of the state of stress in axial direction, the state of shear stress might be also of particular interest, see, for example, (El-Nady and Negm, 2012; Sayyad et al., 2015; Hajianmaleki and Qatu, 2011) and the literature cited therein. Furthermore, the deflection of the beam, which is the result of the externally applied load, is of specific interest because it requires the evaluation of the bending stiffness. The mechanics of multi-layered beams are described using two theories, namely, multi-layer theory and equivalent single layer theory. For more information on multi-layer theory, we refer to (Kao and Ross, 1968; Škec and Jelenić, 2014) and for equivalent single layer theory to (Abrate and Di Sciuva, 2017).

This short contribution summarizes the results of a classical beam theory for long beams, where the layers are assumed to be comprised of linear elastic and isotropic materials. Here, we extend the two-layer approach of (Gross et al., 2007) to an arbitrary number of layers. Of course, the constitutive model can be extended to inelasticity with the consideration of plasticity effects. However, the theory of linear elasticity is a primary indicator of the failure behavior expected later on. This touches upon the question, why not directly treating these multi-layered beams using finite elements? The simplest model should reflect the basic load-bearing behavior and act as an indicator, by which the resulting equations give insight onto the principal response of the structure. Furthermore, the proposed simple theory can be treated in education as well.

In the applied modeling concept the shear deformation is neglected in the first step. However, the shear stresses are considered by approximating the local balance of linear momentum. Later, the shear strains are computable. However, it is known that, for the case of high length to height ratios, they do not have essential influence on the total deflection of the beam.

In the examples shown later on, we investigate MPM beams (metal-polymer-metal) with symmetric and unsymmetrical layer arrangements for various numbers of layers. Here, we show the axial and shear stress distribution along the thickness of the layered beams.

2 A Layered Beam Theory Model

In the following, a beam theory with a finite arbitrary number of layers with different thickness and Young's moduli is derived. In the classical beam theory, the normal (axial) stress distribution is given by

$$\sigma_{xx}(x,z) = -Ew''(x)z, \tag{1}$$

where E represents the Young modulus, $w(x)$ represents the deflection of the beam, x represents the axial coordinate and z represents the coordinate in vertical direction, see Figs. 1 and 2. The basic assumption in the underlying modeling concept is, that the cross-sections deform over the height as a linear function in x-direction, i.e. the axial displacement reads $u(x,z) = -w'(x)z$. In a more sophisticated laminate theories, this assumption is altered, see (El-Nady and Negm, 2012), which takes into consideration also the shear deformation. This, however, is not of interest in the current simplified investigation.

First, we calculate the coordinate system relative to the beam axis, so that the axial normal force $N(x) = 0$ vanishes. If we have a multi-layered beam made out of different materials, the axial stress (1) in each layer reads

$$\sigma_{xx}^{(k)}(x,z) = \sigma_{xx}(x,z) = -E^{(k)}w''(x)z, \tag{2}$$

and these axial stresses vary in each layer. $E^{(k)}$ symbolizes the Young modulus of layer k, $k = 1,\dots,n_\mathrm{L}$ whereas n_L represents the number of layers. We integrate layer-wise the axial stresses (2) to obtain the normal force

$$\begin{aligned} N(x) &= \int_A \sigma_{xx}(x,z)\,\mathrm{d}A = \sum_{k=1}^{n_\mathrm{L}} \int_{A^{(k)}} \sigma_{xx}^{(k)}(x,z)\,\mathrm{d}A^{(k)} = \\ &= -\sum_{k=1}^{n_\mathrm{L}} E^{(k)} b w''(x) \int_{z_U+\sum_{j=1}^{k-1} h^{(j)}}^{z_U+\sum_{j=1}^{k} h^{(j)}} z\,\mathrm{d}z = -bw''(x) \sum_{k=1}^{n_\mathrm{L}} E^{(k)} h^{(k)} z_S^{(k)}, \end{aligned} \tag{3}$$

where $h^{(k)}$ defines the layer thickness of the k-th layer, see Fig. 1, and

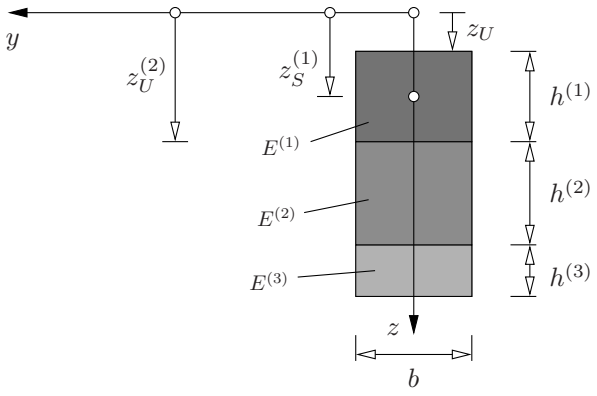

Figure 1: Principal sketch of layered beam (cross section orthogonal to the beam axis)

$$z_S^{(k)} = \frac{1}{h^{(k)}} \int_{z_U+\sum_{j=1}^{k-1} h^{(j)}}^{z_U+\sum_{j=1}^{k} h^{(j)}} z\,\mathrm{d}z = z_U - \frac{h^{(k)}}{2} + \sum_{j=1}^{k} h^{(j)} = z_U + \sum_{j=1}^{k-1} h^{(j)} + \frac{h^{(k)}}{2}, \quad k = 1,\dots,n_\mathrm{L} \tag{4}$$

the center coordinate of each layer. Alternatively, the center of each layer can be expressed by

$$z_S^{(k)} = z_U^{(k)} + \frac{h^{(k)}}{2}, \tag{5}$$

with the upper-edge coordinate

$$z_U^{(k)} = z_U + \sum_{j=1}^{k-1} h^{(j)}, \tag{6}$$

($z_U^{(1)} = z_U$). This leads to the normal force

$$N(x) = -bw''(x) \sum_{k=1}^{n_\mathrm{L}} E^{(k)} h^{(k)} \left(z_U - \frac{h^{(k)}}{2} + \sum_{j=1}^{k} h^{(j)} \right). \tag{7}$$

Since the normal force has to be zero for the cases of pure bending, $N(x) = 0$, the coordinate system can be identified, i.e. the distance to the upper edge z_U is obtained,

$$z_U = \frac{\displaystyle\sum_{k=1}^{n_\mathrm{L}} E^{(k)} h^{(k)} \left(\frac{h^{(k)}}{2} - \sum_{j=1}^{k} h^{(j)} \right)}{\displaystyle\sum_{k=1}^{n_\mathrm{L}} E^{(k)} h^{(k)}} \tag{8}$$

Second, the bending stiffness has to be determined. To this end, the bending moment is calculated by

$$\begin{aligned} M_y(x) &= \int_A \sigma_{xx}(x,z) z \, \mathrm{d}z = -\sum_{k=1}^{n_\mathrm{L}} \int_{A^{(k)}} E^{(k)} w''(x) z^2 \, \mathrm{d}A = \\ &= -w''(x) b \sum_{k=1}^{n_\mathrm{L}} \int_{z_U + \sum_{j=1}^{k-1} h^{(j)}}^{z_U + \sum_{j=1}^{k} h^{(j)}} z^2 \, \mathrm{d}z = -w''(x) \sum_{k=1}^{n_\mathrm{L}} E^{(k)} I_y^{(k)} \end{aligned} \tag{9}$$

with the area moment of inertia in each layer is given by

$$I_y^{(k)} = b \int_{z_U + \sum_{j=1}^{k-1} h^{(j)}}^{z_U + \sum_{j=1}^{k} h^{(j)}} z^2 \, \mathrm{d}z = \frac{b {h^{(k)}}^3}{12} + A^{(k)} {z_S^{(k)}}^2 = \frac{b {h^{(k)}}^3}{12} + b h^{(k)} {z_S^{(k)}}^2, \tag{10}$$

with $z_S^{(k)}$ defined in Eq.(4) and the partial cross section of the k-th layer, $A^{(k)} = b h^{(k)}$. The term $K = \sum_{k=1}^{n_\mathrm{L}} E^{(k)} I_y^{(k)}$ can be interpreted as resulting bending stiffness which leads to

$$M_y(x) = -K w''(x). \tag{11}$$

In combination with the stress state (2), we obtain the axial stress state in the k-th layer of the multi-layered beam as

$$\sigma_{xx}^{(k)}(x,z) = M_y(x) \frac{E^{(k)}}{K} z. \tag{12}$$

If we combine Eq.(11) with the equilibrium conditions $M_y'(x) = Q_z(x)$ and $Q_z'(x) = -q_z(x)$, where $Q_z(x)$ represents the (transverse) shear force and $q_z(x)$ represents the distributed transversal loading, we arrive at

$$K w''''(x) = q_z(x) \tag{13}$$

and

$$Q_z(x) = -K w'''(x). \tag{14}$$

The shear stresses $\tau_{xz}(x,z)$, which determine the shear force $Q_z(x) = \int_A \tau_{xz}(x,z) \, \mathrm{d}A$, are calculated by the local balance of linear momentum,

$$\frac{\partial \sigma_{xx}(x,z)}{\partial x} + \frac{\partial \tau_{xz}(x,z)}{\partial z} = 0 \tag{15}$$

$$\frac{\partial \tau_{xz}(x,z)}{\partial x} = 0 \tag{16}$$

(condition (16) leads to the restriction $Q_z(x) = \mathrm{const.}$, which is commonly ignored to obtain an estimation of the stress state). By introducing the shear flux $T(x,z) := b\tau_{xz}(x,z)$, multiplication of Eq.(15) with the width b, evaluation of $M_y'(x) = Q_z(x)$, insertion of Eq.(12) and the derivative

$$\frac{\partial \sigma_{xx}(x,z)}{\partial x} = M_y'(x) \frac{E^{(k)}}{K} z = Q_z(x) \frac{E^{(k)}}{K} z \tag{17}$$

yields

$$\frac{\partial T(x,z)}{\partial z} = -bQ_z(x)\frac{E^{(k)}}{K}z, \tag{18}$$

where the boundary conditions $T(x,z_U) = T(x,z_L) = 0$ ($z_L = z_U + h$ defines the lower edge) have to be fulfilled since $\tau_{xz}(x,z_U) = \tau_{xz}(x,z_L) = 0$ holds. Integration of Eq.(18) leads to

$$T(x,z) = -bQ_z(x)\int_{z_U}^{z}\frac{E^{(k)}}{K}\zeta\,\mathrm{d}\zeta, \tag{19}$$

which has to be done layer-wise using the upper layer coordinate (6)

$$T^{(k)}(x,z) = -\frac{Q_z(x)b}{K}\left(\left(\sum_{j=1}^{k-1}E^{(j)}\int_{z_U^{(j)}}^{z_U^{(j+1)}}\zeta\,\mathrm{d}\zeta\right) + E^{(k)}\int_{z_U^{(k)}}^{z}\zeta\,\mathrm{d}\zeta\right) \tag{20}$$

or evaluating the integrals

$$\tau_{xz}^{(k)}(x,z) = -\frac{Q_z(x)}{K}\left(\left(\sum_{j=1}^{k-1}\frac{E^{(j)}}{2}\left(z_U^{(j+1)^2} - z_U^{(j)^2}\right)\right) + \frac{E^{(k)}}{2}\left(z^2 - z_U^{(k)^2}\right)\right). \tag{21}$$

3 Examples

As examples, we choose SPS-layers (steel-polymer-steel layers) with symmetric and asymmetric layer arrangement, where we are interested in the evaluation of bending stiffness and the stress distribution along the height in one-, two-, three- and five-layered laminates. Furthermore, the final example considers the influence of fiber reinforcement on the distribution of stress state in the polymer core. All examples concern three-point bending, see Fig. 2, leading to the maximum bending moment and shear force

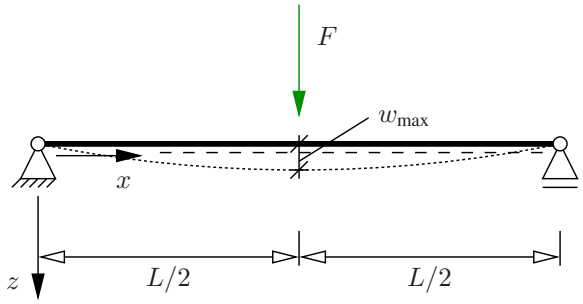

Figure 2: Three-point bending example

$$M_{\max} = M_y(L/2) = F\frac{L}{4}, \quad Q_{\max} = Q_z(L/2) = \frac{F}{2}. \tag{22}$$

For the notation in use, see (Hartmann, 2015). Since we are interested in a displacement-controlled process, the maximum displacement at $x = L/2$ reads

$$w_{\max} = w(L/2) = \frac{FL^3}{48K}, \tag{23}$$

yielding the maximum bending moment and shear force

$$M_{\max} = \frac{12K}{L^2}w_{\max}, \quad Q_{\max} = \frac{24K}{L^3}w_{\max}. \tag{24}$$

For all computations, we draw on a length $L = 100\,\mathrm{mm}$, a width of $b = 20\,\mathrm{mm}$. Both quantities are required in Eqns.(12) and (21).

3.1 Symmetric Layer Arrangement

As first examples, we look at the bending stiffness and stress states of multi-layered metal sheets with symmetric layer arrangement as applied in (Harhash et al., 2018). Here, we obtain the bending stiffness for different layers according to Tab. 1, and the center coordinate system defined by the upper-edge coordinate z_U. Fig. 3(a) shows the

Table 1: Origin of the coordinate system relative to upper edge, and bending stiffness for various laminates (steel: $E_s = 196\,054\,\mathrm{N\,mm^{-2}}$; polymer: $E_p = 1517\,\mathrm{N\,mm^{-2}}$)

SPS mm	z_U mm	K/b Nmm	required force N
0.49/0/0	-0.245	1922	1.85
0.49/0/0.49	-0.49	15377	14.76
0.49/0.3/0.49	-0.64	33825	32.47
0.49/0.6/0.49	-0.79	60940	58.50
0.49/1.0/0.49	-0.99	110609	106.19
0.49/2.0/0.49	-1.49	302666	290.56

distribution of axial stresses (12) along the height for the SPS-configurations detailed in Tab. 1, which are shown

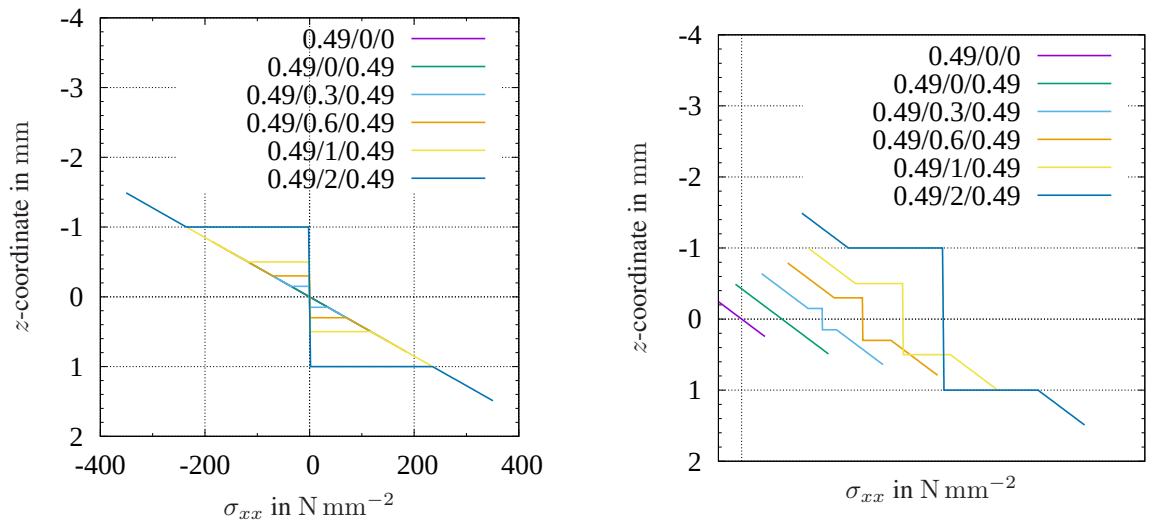

(a) Axial stress $\sigma_{xx}(L/2, z)$

(b) Axial stress resolved in detail $\sigma_{xx}(L/2, z)$

Figure 3: Axial stress distribution of symmetric layer arrangements for given maximum displacement $w_{\text{max}} = 1\,\mathrm{mm}$

for $w_{\text{max}} = 1\,\mathrm{mm}$. It must be mentioned that the "layer indicator" 0.49/0/0 implies one steel layer with a thickness of $0.49\,\mathrm{mm}$ (no further layers), and 0.49/0/0.49 means that there is no polymer core.

In order to see the distribution in more detail, Fig. 3(b) shows the axial stress state in an exploded diagram. Obviously, due to the low value of Young's modulus and the location of the polymer core in the multi-layered beams, the axial stresses are very small. Most of the load is transmitted by the outer steel layers. However, if we look at the shear stress distribution (21), see Fig. 4, it is different. The highest values of shear stress are in the polymer core material, although there is no essential shear load contribution by the "weak" layer. This affects essentially the contact between the polymer and steel. Furthermore, we can observe that for given displacements w_{max} the required forming force F, see Eq.(23), increases with increasing bending stiffness K, see Tab. 1 as well.

3.2 Fiber Reinforcement

There exist composite materials where the polymer core is reinforced with glass fibers. For the current scenario, we assume that the reinforced composite has a volume fraction of 50% with a Young's modulus of glass fibers

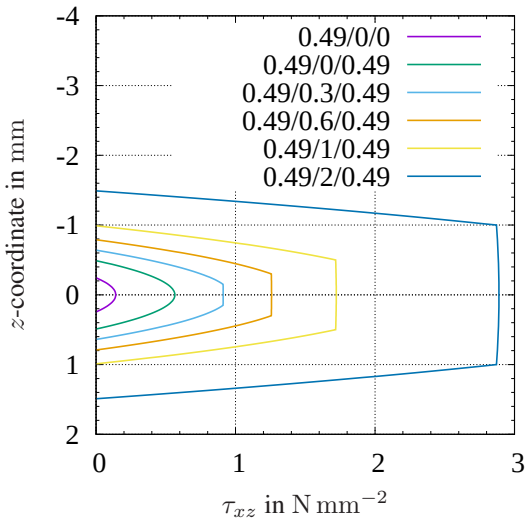

Figure 4: Maximum shear stress distribution τ_{xz} for symmetric layer arrangements, see SPS-configurations of Tab. 1

$E_f = 75\,000\,\mathrm{N\,mm^{-2}}$ and the matrix material has a Young's modulus of $E_m = 2000\,\mathrm{N\,mm^{-2}}$. The placement of fibers are parallel to the longitudinal direction of the beam. If we draw on the Rule of Mixtures (ROM), the resulting Young's modulus of the composite ply reads

$$E = \frac{V_f}{V} E_f + \frac{V_m}{V} E_m = 38\,500\,\mathrm{N\,mm^{-2}}, \tag{25}$$

where the volume fractions $V_f/V = V_m/V = 0.5$ are identical.

In the following, we compare an SPS-system 0.49/1/0.49 with and without glass-fiber reinforcement. The bending stiffness for a pure matrix material is $K = 2\,212\,990\,\mathrm{N\,mm^2}$ and with fiber reinforcement $K = 2\,273\,823\,\mathrm{N\,mm^2}$, i.e. the fiber reinforcement does not have an essential contribution to the bending stiffness. Fig. 5 shows the axial

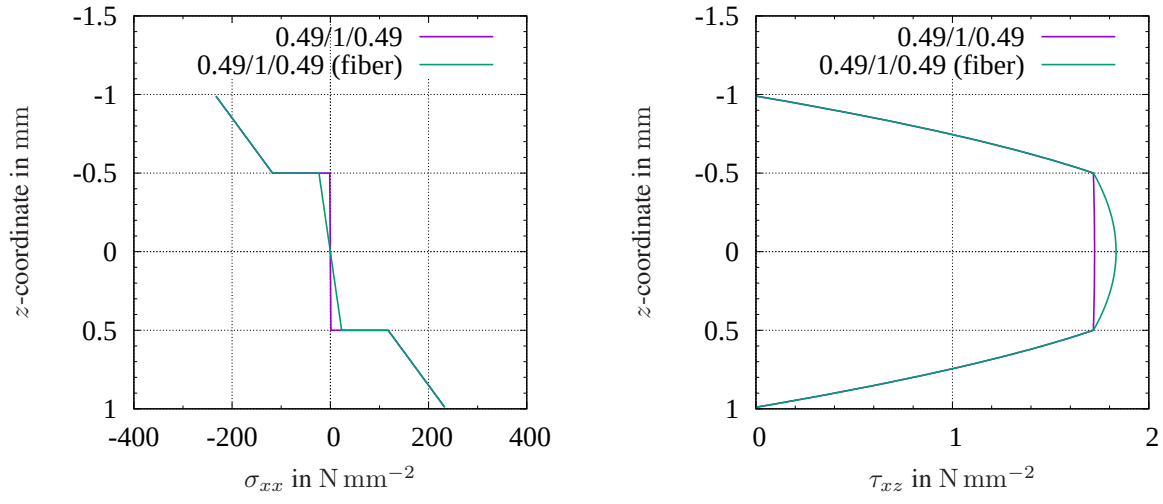

(a) Axial stress $\sigma_{xx}(L/2, z)$

(b) Shear stress $\tau_{xz}(x, z)$

Figure 5: Comparison of an SPS-system 0.49/1/0.49 with pure matrix material and fiber reinforcement

and shear stress distribution in a multi-layered beam with and without fiber reinforcement. The shear stresses are

comparatively larger at the center of the reinforced composite core, i.e. they affect the core material to a greater extent.

3.3 Unsymmetrical Layer Arrangement

Not only the symmetric, but also an unsymmetrical layer arrangement might be of interest, see (Harhash et al., 2018). For the notation in use, e.g. 0.24/0.3/0.49, the first layer of thickness $0.24\,\mathrm{mm}$ is on the upper side (where the load is applied in the three-point bending problem). Tab. 2 compiles four variants of three-layer arrangements,

Table 2: Origin of the coordinate system relative to upper edge, and bending stiffness for various laminates for unsymmetrical layer arrangement (steel: $E_s = 196\,054\,\mathrm{N\,mm^{-2}}$; polymer: $E_p = 1517\,\mathrm{N\,mm^{-2}}$)

SPS(PS) in mm	z_U in mm	K/b in Nmm
0.49/0.3/0.24	-0.46	16132
0.24/0.3/0.49	-0.57	16132
0.24/0.6/0.49	-0.77	31634
0.49/0.6/0.24	-0.56	31634
0.49/0.3/0.24/0.3/0.24	-0.71	50903
0.24/0.3/0.24/0.3/0.49	-0.86	50903

where, of course, for the same choice of layer thicknesses, the bending stiffness K is identical. However, the normal stress distribution, see Fig. 6 is different. The shear stress concerned are depicted in Fig. 7 showing again

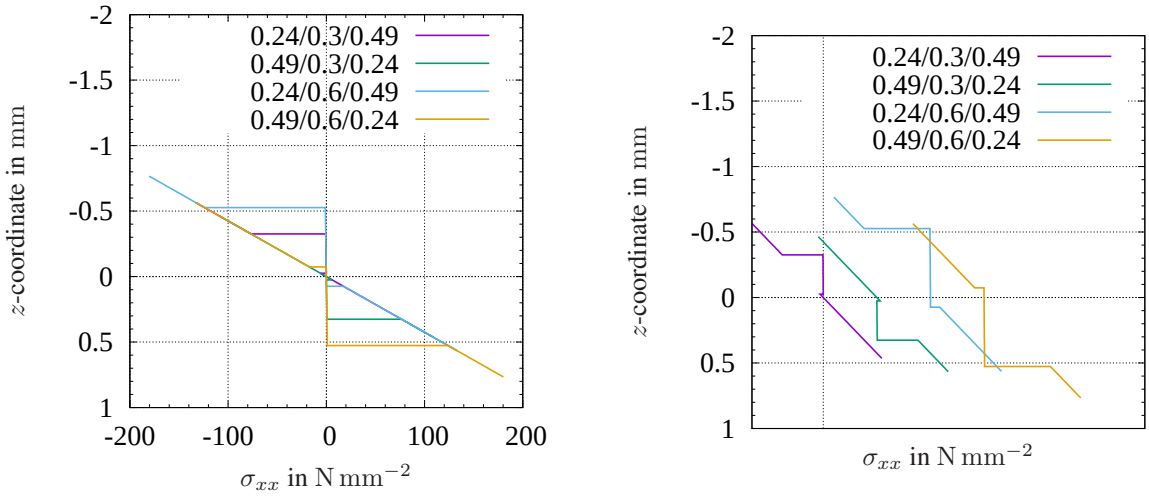

(a) Axial stress $\sigma_{xx}(L/2, z)$

(b) Axial stress resolved in detail $\sigma_{xx}(L/2, z)$

Figure 6: Axial stress distribution of unsymmetrical layer arrangements for given maximum displacement $w_{\max} = 1\,\mathrm{mm}$

that the maximum shear stresses occur within the polymer layer.

Finally, we consider two variants of unsymmetrical layer arrangement of five layers, see Fig. 8. For the case of $0.49/0.3/0.24/0.3/0.24$ the tensile stresses are much larger than for the opposite case, and, thus, are more critical.

4 Conclusions

We recap the classical beam theory for compound beams comprised of two-layered beams and extend the equations of mechanics to an arbitrary number of layers with different elastic properties and thicknesses. The formulas can directly be programmed to obtain the results for the center of coordinate system, area moment of inertia, bending stiffness and the axial and the shear stress state in each layer. The equations show the experienced-based

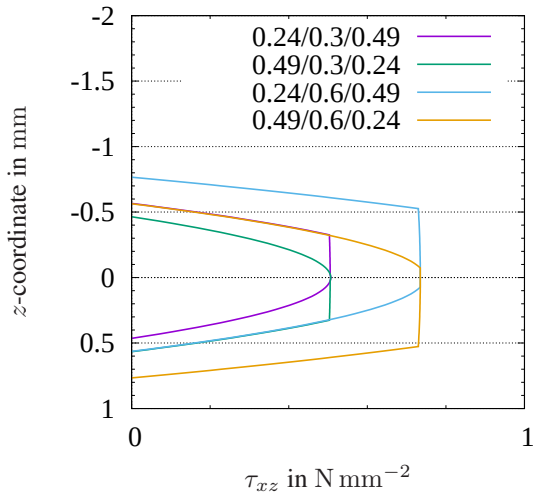

Figure 7: Maximum shear stress distribution τ_{xz} for unsymmetrical layer arrangements, see SPS-configurations of Tab. 2

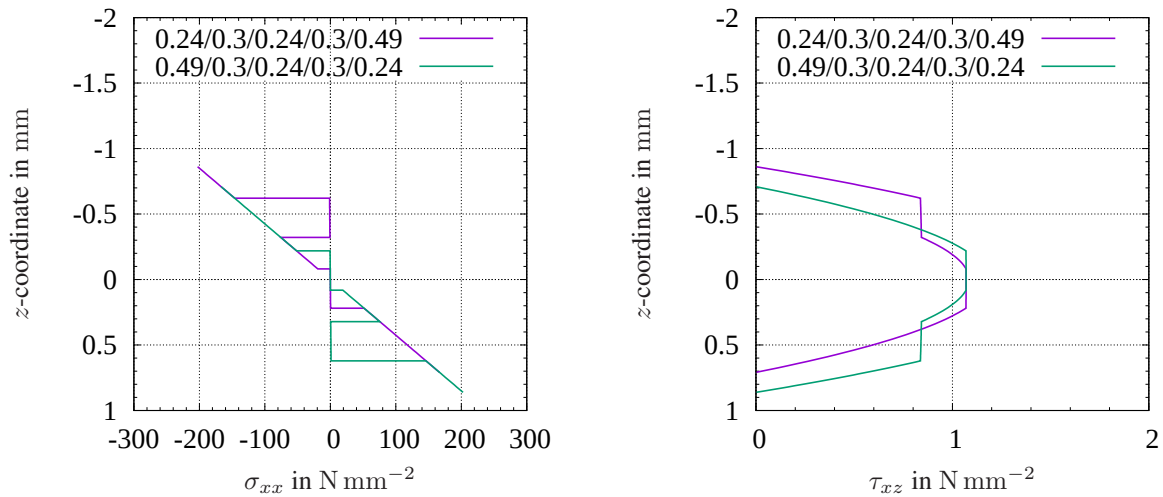

(a) Axial stress $\sigma_{xx}(L/2, z)$

(b) Shear stress $\tau_{xz}(x, z)$

Figure 8: Stress distribution of unsymmetrical, five-layered SPSPS-systems

knowledge that most of the normal stresses are affecting the steel components in SPS configuration. However, the shear stresses have their maximum values in the polymer core components. As a first indicator of the load-bearing parts, the analytical formulas are very helpful.

Acknowledgment

We gratefully acknowledge the financial support provided by the German Research Foundation DFG (Grant No HA 2024/19-1) to fund this research.

References

Abrate, S. and Di Sciuva, M. (2017). Equivalent single layer theories for composite and sandwich structures: A review. *Composite Structures*, 179.

Burchitz, I., Boesenkool, R., van der Zwaag, S., and Tassoul, M. (2005). Highlights of designing with hylite – a new material concept. *Materials & Design*, 26(4):271–279.

Carrera, E., Giunta, G., and Petrolo, M. (2011). *Beam structures: classical and advanced theories*. John Wiley & Sons.

De Vries, W. R. and Lauderbaugh, L. K. (1984). A model for bending bimetallic strip. *Journal of Engineering for Industry*, 106:62–69.

El-Nady, A. O. and Negm, H. M. (2012). Analysis of arbitrarily laminated composite beams using Chebyshev series. *International Journal of Composite Materials*, 2(5):72–78.

Euler, L. (1744). *Methodus inveniendi lineas curvas maximi minimive proprietate gaudentes*. apud Marcum-Michaelem Bousquet.

Gross, D., Hauger, W., Schröder, J., and Wall, W. (2007). *Technische Mechanik 2, Elastostatik*. Springer, Berlin, 9th edition.

Hajianmaleki, M. and Qatu, M. S. (2011). Mechanics of composite beams. In Tesinova, P., editor, *Advances in Composite Materials - Analysis of Natural and Man-Made Materials*, chapter 22, pages 527–546. Intech Europe, Rijeka, Croatia.

Harhash, M., Gilbert, R. R., Palkowski, H., and Hartmann, S. (2018). Experimental characterization, analytical and numerical investigations of metal/polymer/metal sandwich composites – part 1: Deep drawing. *Composite Structures*, 202:1308 – 1321.

Hartmann, S. (2015). *Technische Mechanik*. Wiley-VCH, Weinheim, Germany, 1st edition.

Hufenbach, W., Jaschniski, J., Weber, T., and Weck, D. (2008). Numerical and experimental investigations on HYLITE sandwich sheets as an alternative sheet metal. *Archives of Civil and Mechanical Engineering*, 8(2):67–80.

Kao, J.-S. and Ross, R. J. (1968). Bending of multilayer sandwich beams. *AIAA Journal*, 6(8):1583–1585.

Labuschagne, A., van Rensburg, N. J., and Van der Merwe, A. (2009). Comparison of linear beam theories. *Mathematical and Computer Modelling*, 49(1-2):20–30.

Leichti, R. J., Falk, R. H., and Laufenberg, T. L. (1990). Prefabricated wood composite I-beams: a literature review. *Wood and Fiber Science*, 2(1):62–79.

Sayyad, A. S., Ghugal, Y. M., and Naik, N. S. (2015). Bending analysis of laminated composite and sandwich beams according to refined trigonometric beam theory. *Curved and Layered Structures*, 2:279–289.

Škec, L. and Jelenić, G. (2014). Analysis of a geometrically exact multi-layer beam with a rigid interlayer connection. *Acta Mechanica*, 225(2):523–541.

Timoshenko, S. P. (1921). On the correction for shear of the differential equation for transverse vibrations of prismatic bars. *The London, Edinburgh, and Dublin Philosophical Magazine and Journal of Science*, 41:744–746.

Timoshenko, S. P. (1922). X. on the transverse vibrations of bars of uniform cross-section. *The London, Edinburgh, and Dublin Philosophical Magazine and Journal of Science*, 43(253):125–131.